NEARSHORE BARS AND SHORELINE DYNAMICS ASSOCIATED WITH THE IMPLEMENTATION OF A SUBMERGED BREAKWATER: TOPO-BATHYMETRIC ANALYSIS AND VIDEO ASSESSMENT AT THE LIDO OF SÈTE BEACH

Bouvier[1,2], C., Balouin[1], Y. and Castelle[2], B.

Abstract

Accurate topo-bathymetric data and video imagery analysis are combined to investigate the impact of the implementation of a 1-km long submerged breakwater on sandbar and shoreline dynamics at the microtidal wave-dominated beach of Sète, SE France. The topo-bathymetric analyses are used to quantify sand volume associated with morphological changes and the video imagery is used to address the high-frequency response of the sandbar-shoreline geometry. While the structure is found to reduce erosion and submersion hazards, our results also indicate that the structure had a profound impact on the coupled shoreline-sandbar system, particularly onshore of the breakwater. This impact cascades alongshore and deeply modified the nearshore system dynamics a few kilometers away from the structure. A progressive rotation and linearization of the sandbar was observed shoreward of the submerged breakwater. This resulted in the splitting of the sandbar adjacent to the structure during an episodic net offshore sandbar migration event. The typical formation of a salient or tombolo was not observed. Instead, shoreline coupled to the sandbar geometry, which resulted in a slight seaward migration of the shoreline in front of the structure.

Key words: nearshore sandbars, shoreline, submerged structure, coastal morphodynamics

1. Introduction

Coastal protection hard structures such as groynes, breakwaters, seawalls and revetments have been implemented worldwide to limit coastal erosion and to provide flooding protection to the hinterland (Ranasinghe and Turner, 2006). However, this traditional coastal defence strategy is increasingly unpopular as it is costly and lastingly scars the landscape. Coastal management practices nowadays no longer rely solely on hard coastal defence structures. Soft options like beach nourishments are increasingly preferred (e.g. Hamm et al. 2002; Charlier et al., 2005; Castelle et al., 2009) or more rarely using of soft submerged structure. Shoreface nourishments have been studied extensively as they are a common practice nowadays in many countries worldwide, such as in the Netherland (Grunnet and Ruessink, 2004). In contrast and despite their logic and benefit, the influence of soft submerged structures has received little attention in the scientific literature (Black, 2001; Evans and Ranasinghe, 2001). Noteworthy, all the literature on submerged structures, including field observation and modelling, have dealt with their impact on shoreline response and systematically overlooked their impact on the nearshore sandbar(s). Beside their fundamental scientific interest, sandbars play a key role in coastal protection during storm, dissipating wave energy before they reach the shore. Moreover, nearshore sandbars potentially enforce alongshore morphological variability at the beach, up to the shoreline and the coastal dune (e.g., Thornton et al., 2007; Van de Lageweg, 2013; Castelle et al., 2015).

Morphological changes on wave-dominated barred beaches are challenging to address as they cover a wide range of spatial and temporal scales. Shallow-water morphological changes on the timescales from hours (storms) to years through seasons and months are primarily driven by breaking-wave-induced hydrodynamics. Traditional topo-bathymetric measurements cannot address this wide range of scales,

[1] BRGM, Occitanie-Pyrénées-Méditerranée (SGR/LRO), 1039 Rue de Pinville, 34000 Montpellier, France

[2] UMR CNRS 5805 EPOC « Environnements et Paléoenvironnements Océaniques et Continentaux, Allée Geoffroy Saint-Hilaire, CS 50023, 33615 Pessac Cedex, France

Corresponding author: c.bouvier@brgm.fr

mostly because of the cost and the practical difficulties to survey the nearshore. Instead, video monitoring, which optically remotely sense the breaking waves and the beach can provide daily data of the geometry of the shoreline (through the high color contrast between water and sand) and the sandbar(s) (through high-intensity depth-induced breaking wave patterns). Although it has rarely been done in the scientific literature, the combination of numerous topo-bathymetric data and video monitoring can provide outstanding insight into the nearshore system behavior. The objective of this paper is to extensively describe the influence of a recently deployed submerged breakwater on sandbar and shoreline dynamics at a microtidal wave-dominated sandy beach (Sète, SE France). We use topo-bathymetric data to describe morphological changes following breakwater deployment and 5 years of video images, including 3 years after the deployment, to address the high-frequency response of the shoreline-sandbar system.

2. Field site

The Lido of Sète is a narrow coastal barrier facing the Mediterranean Sea located in the northern part of the Gulf of Lions (figure 1a). The studied coast, between Cap d'Agde and Sète is a semidiurnal microtidal environment, with a moderate-energy modal wave climate and episodic severe storms. The coast is exposed to dominant offshore winds. Onshore winds are occasionally observed in autumn and winter during marine storms. Storm events are typically characterized by significant wave heights larger than 3 m, peak wave period around 8 s with an ESE direction, although severe storms from the S can be observed.

The lido of Sète is characterized by a double bar system. The relatively alongshore-uniform outer bar is located between 250 m and 400 m from the shore with its crest in approximately 4 m below mean sea level. The inner bar is mainly crescentic with an oblique configuration (Aleman, 2013), i.e. attached to the shore in the northeastern sector and progressively detaching southwards to reach a distance of approximately 170 m from the shore at the end of the southwestern sector. The typical inner bar crest depth is 2 m below mean sea level. The averaged mean shoreface slope is 0.9 % with a mean grain size of approximately 200 μm (Certain, 2002). The shoreline is mostly non-uniform alongshore due to protruding megacusps enforced by the offshore bar with a mean wavelength of 400 m (Balouin, 2013).
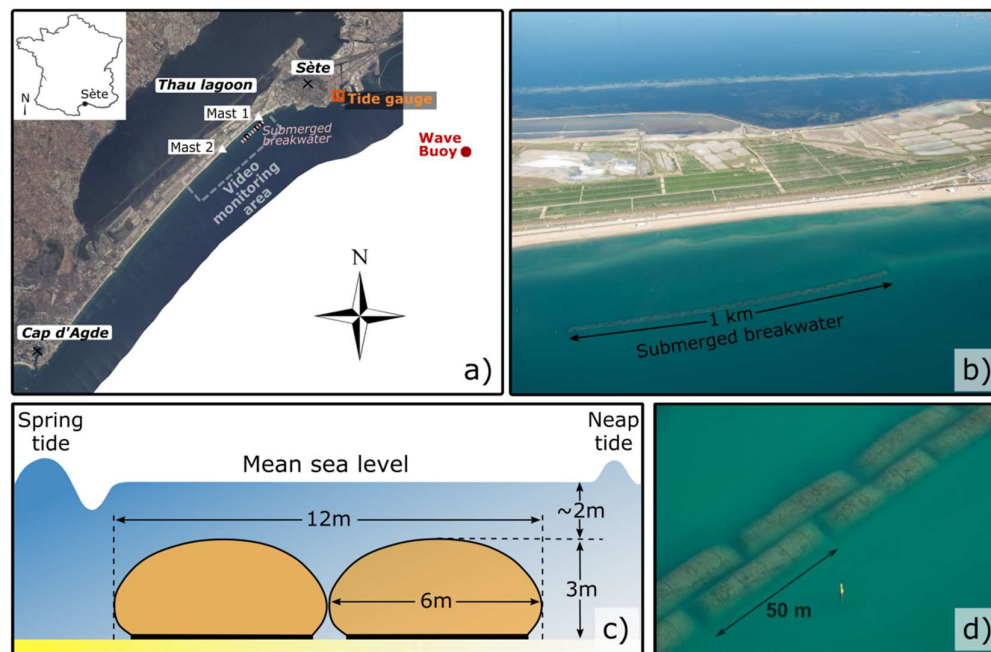

Figure 1. Map of the study site including the position of submerged breakwater, wave buoy, tide gauge and masts were cameras are installed (a). Dimension and aerial views of the submerged breakwater containers (b, c and d).

The Lido of Sète has experienced chronic marine erosion during the last decade, with a 50-m beach retreat in less than 50 years (Certain and Barusseau, 2005). This is particularly problematic as the beach system is of major interest from the perspective of socio-economic activity as it is a major international and national tourism destination with beach attendance up to 1 million per year (Balouin, 2014). A large beach management program was developed in the Lido to fight against chronic erosion (BCEOM, 2001). The program involved relocating the coastal road several hundred meters inland, widening the beach and building an artificial dune. Simultaneously, a submerged breakwater was installed. The submerged breakwater was implemented in early 2013 on the subdued outer bar located 350 m from the shore (figure 1b). The breakwater consists in 2 50-m long and 6-m wide rows of sand containers (figure 1c and d), extending 800 m and 12 m in the alongshore and cross-shore direction, respectively. It is 3-m high, that is, with its crest in approximately 2-m depth. To finalize coastal management, a beach nourishment of 510 000 m³ of sand has been realized in December 2014 behind the geotube, which has been extended to 1-km long in October 2015.

3. Data acquisitions

3.1. *Wave data*

Incident wave conditions were collected every 30 min from a directional wave buoy located offshore of Sète (Wave Buoy in figure 1a), which was moored in 30 m-depth in January 2011 and recorded data since then. Because the measured time series is interspersed due to a number of brief buoy malfunctions, the dataset was combined with numerical model outputs. Dicca Model (Besio et al., 2016) and the wave forecasting system developed by Puertos Del Estado (Gomez Lahoz and Carretero Albiach 2005) were used before and after 2014, respectively. Compared to measured data, root mean square error in significant wave height Hs and peak wave period Tp is smaller than 0.3 m and 1.3 s, respectively. The wave direction of the moderate- to high-energy events is also well reproduced. The wave component of the longshore energy flux per unit length of beach was calculated with θ the angle of wave incidence with respect to shore normal, and P the available wave power per unit length measured in Kilowatt per meter evaluated using the measured spectral Hs (Longuet-Higgins, 1971):

$$P_l = P.sin\theta.cos\theta \ [kW/m] \tag{1}$$

3.2. *Topographic and bathymetric survey*

The three topo-bathymetric surveys (November and December 2013, June 2016) consist of a series of echo sounding data spaced at an alongshore distance of approximatively 30 m. Each survey point is estimated to have a vertical and horizontal accuracy of ± 5 cm and 1 m, respectively. Digital terrain models (DTM) were created for each survey by interpolation of the bed level measurements using triangulation with linear interpolation. The bathymetric data is completed by three high-resolution topo-bathymetric LiDAR imageries (2009, 2011 and 2014). The bathymetric beam frequency is 900 Hz for a minimal spatial resolution around 5 m and a vertical accuracy of about 30 cm. The collected data extend from the wooden stacks positioned on the dune foot to 20 m water depth in the cross-shore direction and along 3.5 km alongshore. A total of 6 accurate topo-bathymetries is therefore analyzed in this paper.

3.3. *Video data*

An Argus video monitoring system (Holman and Stanley, 2007) consisting in 8 cameras mounted on two 20-m high 2.5-km spaced has been collecting data since mid-April 2011. 10-min averaged images of the 8 cameras were combined and transformed to real-world plan view images (Holland et al. 1997) on a 2 x 2 m grid from April 2011 to April 2016. The rectified images extend 600 m in the cross-shore (Xargus) and 4 km in the alongshore (Yargus) direction (figure 2). In the bar area in front the station locations (Yargus = 0 and Yargus = - 2500), the maximum pixel footprint is 2 and 0.5 m in the cross-shore and alongshore directions respectively. These accuracies worsen to about 5 and 30 m at the southwestern end of the field

site. Morphological features (bar, shoreline) were extracted using ARGUS toolboxes (Holman and Stanley, 2007, Pape, 2008) through the sampling of pixel luminosity intensity (Lippmann and Holman, 1990). The maximum pixel intensity is a good proxy for the submerged sandbars position. Alongshore-averaged sandbar positions were computed in two different geographic sectors: within the 1.3 km-long NE sector located in front of submerged structure (Yargus = 1250 to 2550 m) and within the 1.5 km-long SW (Yargus = -1000 to 500 m). The alongshore sections length well exceeds the alongshore wavelength of crescentic sandbar and megacusps, which influence is therefore filtered when computing the alongshore-averaged parameters. Cross-shore positions were computed from the wooden stacks positioned on the dune foot that constitutes a fixed reference. Sandbar obliquity and three-dimensionality were computed in the NE sector (Yargus = 1250 to 2550 m) facing submerged structure. Obliquity was estimated through the angle between wooden stack line and the linear regression of the sandbar. Three-dimensionality (α) was computed through the alongshore standard deviation between the sandbar and its linear regression. The shoreline position was extracted approximately every 15 days for low-energy wave conditions to limit the wave-set-up-induced errors. Beach width was computed from the dune foot.
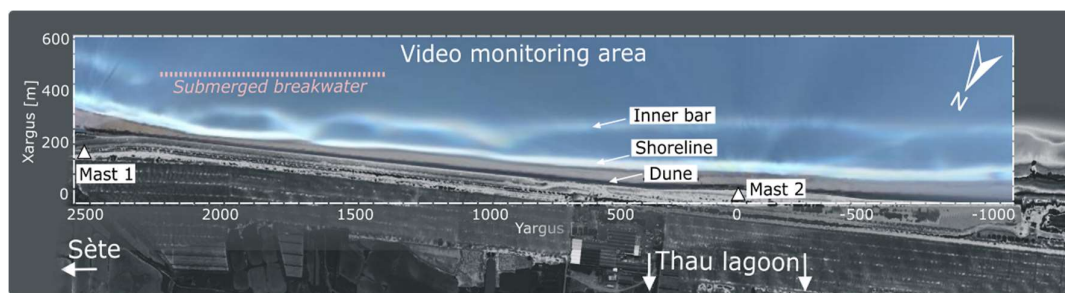

Figure 2. Planview time-exposure image (23 October 2011).

4. Results

4.1. Overall sandbar-shoreline behavior before and after the breakwater implementation

Before the breakwater implementation in 2013 two nearshore bars were present in the study area (figure 3a and b). The linear outer bar, which was well-developed in the NE sector (Yargus = 2550 to 1250 m), was slowly decaying decaying in the seaward region of the nearshore in the SW sector (Yargus = 500 to -1000 m). The outer bar was located between 250 to 400 m from the shore with its crest in approximately 3 to 4 m below mean sea level. In the NE sector, the inner bar was close to the shore with well-developed crescentic patterns almost attached to the beach with a mean wavelength of 400 m. In contrast, in the SW sector the inner bar was located approximately 200 m from the shoreline in the SW sector with a more alongshore-uniform shape. The inner bar crest reached 0.6 m bellow mean sea level near the horn in the NE sector while crest in SW sector was in approximately 2-m depth. During the same period, the inner bar showed quite large cross-shore and alongshore variability. Shoreline-sandbar coupling was also observed with shoreline megacusp embayments facing the sandbar bays.

   The implementation of the structure in early 2013 had a profound impact on the inner-bar morphology. A progressive linearization and rotation of the inner bar becoming parallel to the tube was observed in the NE sector (figure 3c, d, e and f). In the SW sector, the inner bar pursued its offshore migration. The combination of both alongshore and cross-shore evolutions drove the split of the sandbar at the end of 2013 (figure 3d). The strong offshore migration of the sandbar in the SW sector yielded to the progressive formation of a new inner bar close to the shoreline (Net Offshore Migration – NOM - cycle) that subsequently rapidly realigned to the inner bar of the NE sector (figure 3c, d, e and f). Shoreline-sandbar coupling was still observed after the implementation of the submerged breakwater with the disappearance of shoreline rhythmicity associated to the inner sandbar linearization. Figure 3f shows the beach morphology 19 months after the beach nourishment. The sand was initially deposited on beach facing the submerged breakwater area, but an important volume rapidly migrated offshore in shallow water.
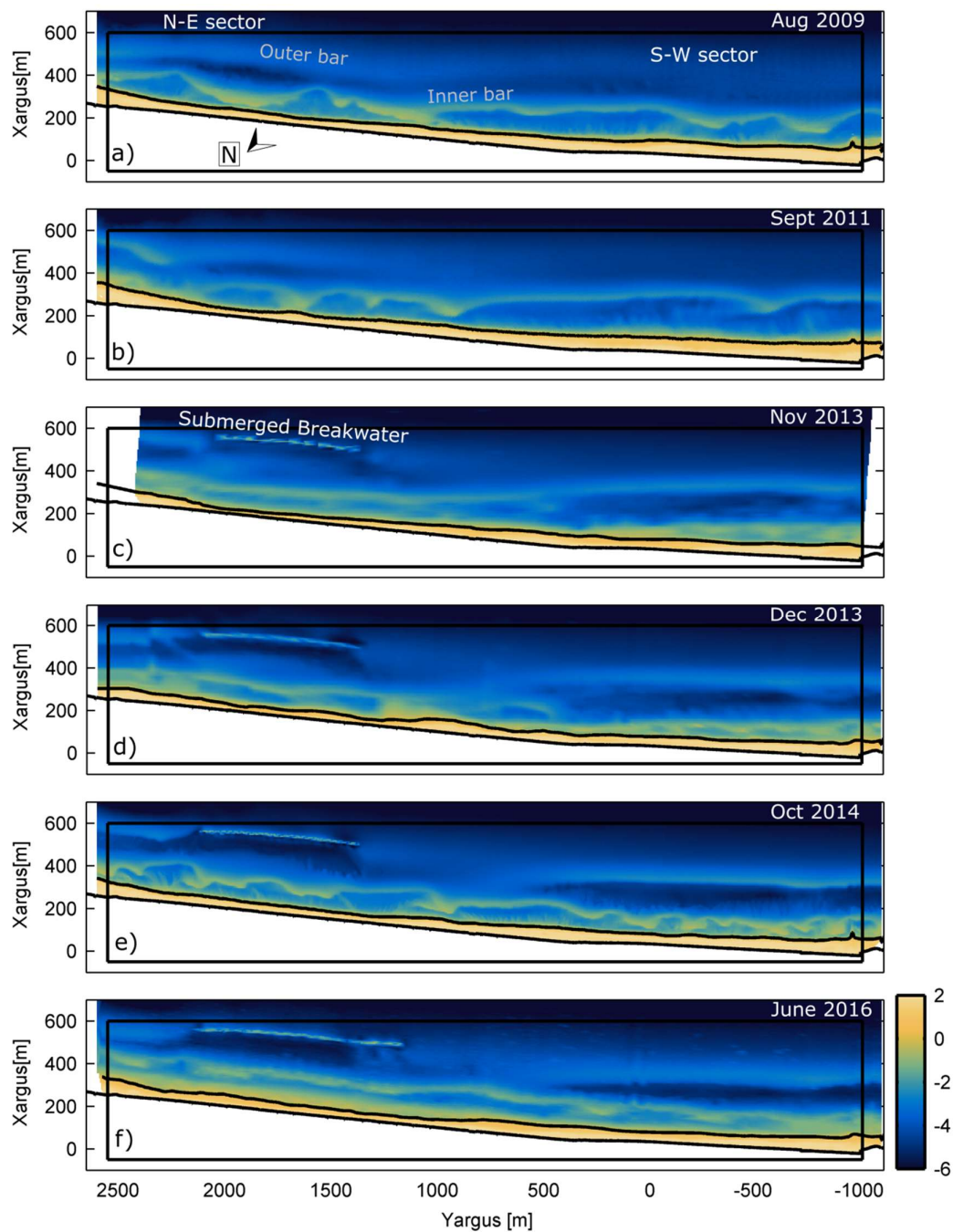
Figure 3. Plan view of the nearshore bathymetry: a) August 2009, b) September 2011, c) November 2013, d) December 2013, e) October 2014 and f) June 2016.In all panels the black lines indicate the wooden stacks and shoreline position.

To complete the analysis on the beach response to the submerged breakwater deployment, the difference plot in bathymetry between the pre- and post-breakwater deployment data is given in figure 4 (November 2013 with September 2011). Large erosion/accretion patterns (between +2 and -3 m) are observed. Erosion and accretion patterns at the inner bar alternate alongshore as a result of the reshaping of the inner bar into a reasonably alongshore-uniform ridge of sand. Important scouring was observed just onshore of the

breakwater. At the NE side of the geotube accretion was observed and reveals an alignment of outer sandbar to the geotube. Accretion was also observed more onshore in the surf zone between Yargus = 1700 to 2550 m which reflects an offshore migration of the inner bar and, as a result, its clockwise rotation. In the SW sector, reasonably alongshore-uniform erosion/accretion patterns reflect the offshore migration of the outer bar. Overall, the difference plot shown in figure 4 highlights that most of the morphological changes occurred in the nearshore, with much more subtle changes at the beach.
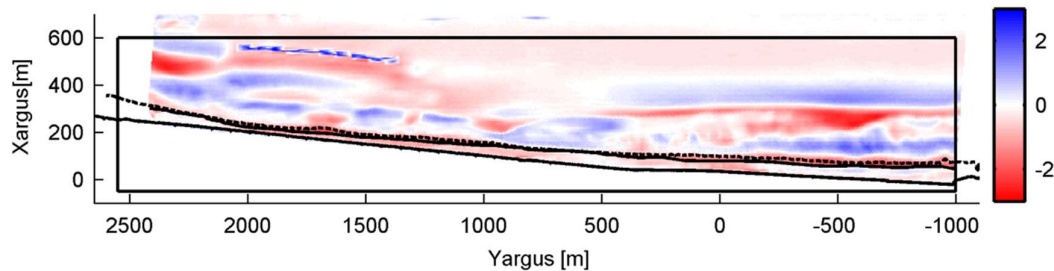

Figure 4. Difference bathymetric plot before and after submerged breakwater deployment (September 2011 vs November 2013).

4.2. Profile response

An illustration of the detailed morphological changes (beach profiles) across the breakwater and the adjacent coast is shown in figure 5. The submerged breakwater was implemented 70 m offshore of the outer bar crest (figure 5a). Clearly, the sandbar disappeared after the implement of the breakwater with a 2-m erosion immediately offshore of the breakwater, while most of the sand appeared to move onshore to form a large sandbar (figure 5a). The cross-shore inner sandbar position remained reasonably stable until nourishment when the sandbar enlarged and migrated almost 50 m offshore. Prior to the breakwater, chronic shoreline erosion was observed, but this trend reversed in December 2013 with an advance of 25 m in 1 year. On shorter timescales, the beach rapidly enlarged by approximately 15 m between November and December 2013. This accretion was unexpected given that between the 2 bathymetries of winter 2013, the beach was submitted to a 4.7 Hs_{max} storm. After nourishment in December 2014, a shoreline accretion by 10 m and a substantial decrease in beach slope was observed.

On the adjacent coast, an offshore migration and increase in depth of the (initial) inner bar is clearly observed throughout the study period (figure 5b). At the end of the study, the new inner sandbar was located 100 m further offshore from its initial position and was nearly 1 m less high. A new nearshore sandbar was created in 2013, concurrent with a 15-m shoreline retreat, which migrated offshore to progressively replace the former.
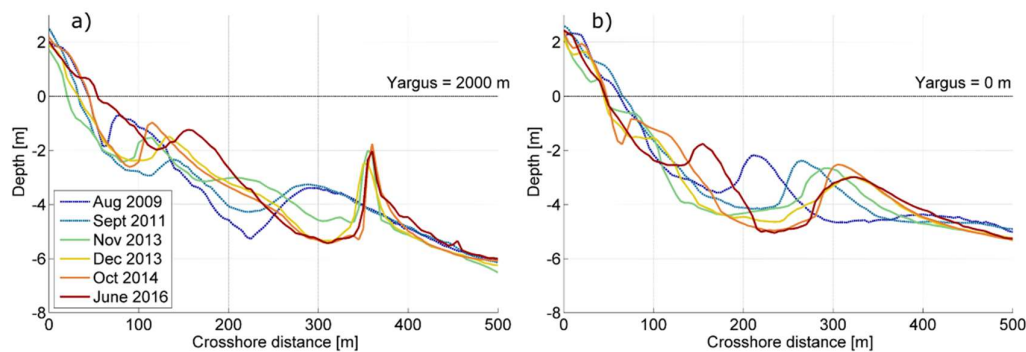

Figure 5. Depth versus crosshore distance, here shown for km-section Yargus = 2000 m and for Yargus = 0 m.

4.3. Wave forcing and high-frequency video-derived morphological evolution

5-year continuous video monitoring (2 years prior and 3 years after structure deployment) at Sète is a unique dataset to complete at high-frequency the analysis of the morphological response of the nearshore system to a significant anthropic perturbation introduced by a submerged breakwater. Inner bar crest positions were extracted before and after every significant energetic event (defined as Hs > 1.5 m for at least 12 h). With 72 such events recorded from January 2011 to April 2016, only 59 couples of pre/post storm event video images were analyzed because of camera malfunctions or bad quality images. An example of timex image is given at the beginning of submerged breakwater deployment and 2 years after for same Hs conditions (figure 6). As described with the bathymetric data, video images exhibit sandbar rotation, linearization behind breakwater, offshore migration and splitting on the adjacent coast.

4.3.1. Longshore sandbar response behind submerged structure
The 5-year time series of the alongshore sandbar position in the NE sector together with that of the sandbar three-dimensionality and sandbar obliquity computed with video monitoring data set is given in figure 7d, e and f respectively. Wave conditions (Hs, Tp), total energy P and longshore energy flux Pl are presented in order to associate morphological evolution to hydrodynamic conditions at the beach of Sète (figure 7a, b and c). At the beginning of the study, sandbar was attached to the coast near Yargus = 2250 m (figure 7d) and progressively detached south-westward near Yargus = 1500 m with well-developed crescents with a wave length of 400 m. The bar behind the submerged breakwater before deployment had an angle to the dune of approximatively 2° (figure 7f). Sandbar obliquity remained stable before the structure deployment but longshore migration of the sandbar sinuosity according to longshore energy flux induced by storm waves can be observed (figure 7d). A series of SE storms in October-November 2011 and 2013 period (Pl < 0 in figure 7c) drove longshore migration of 3D pattern toward SW. The temporal evolution of sandbar obliquity shows a significant decay after the structure deployment near January 2013 (figure 7f). The sandbar progressively rotated clockwise to finally become parallel to the dune and so to the breakwater few months after deployment. The process of sandbar rotation is apparently due to an offshore sandbar migration at the North-Eastern boundary of the structure (Yargus = 2250 m to 2500 m in figure 7d). At this location, the sandbar migrated offshore during storm events (March and December 2013 or April 2014). This alongshore variability of cross-shore migration processes induced the process of sandbar rotation described in the first analysis. Even if a tendency of three-dimensionality evolution is not obvious in figure 7e, the timestack in figure 7d clearly shows that the initial 3D patterns were smoothed out after deployment. Some alongshore variability could occasionally develop shoreward of the submerged breakwater (near Yargus = 2250 m) for moderate wave in April 2014 which created an increase in sandbar three-dimensionality. The 4.2 m Hs storm in December 2013 induced a real break in sandbar evolution with the complete sandbar linearization and an apparent offshore migration.
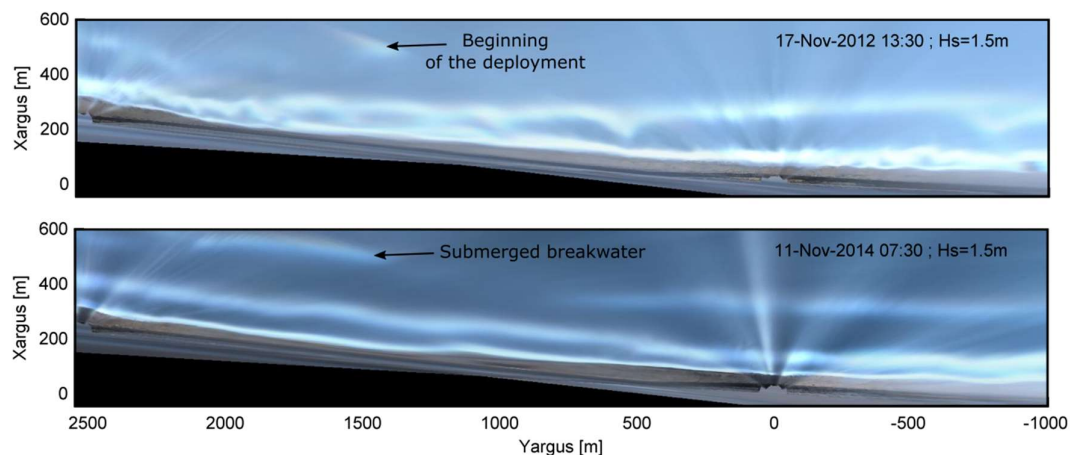

Figure 6. Planview time-exposure images showing sandbar(s) position at the beginning of the deployment (upper panel) and 2 years after submerged breakwater installation (bottom panel).
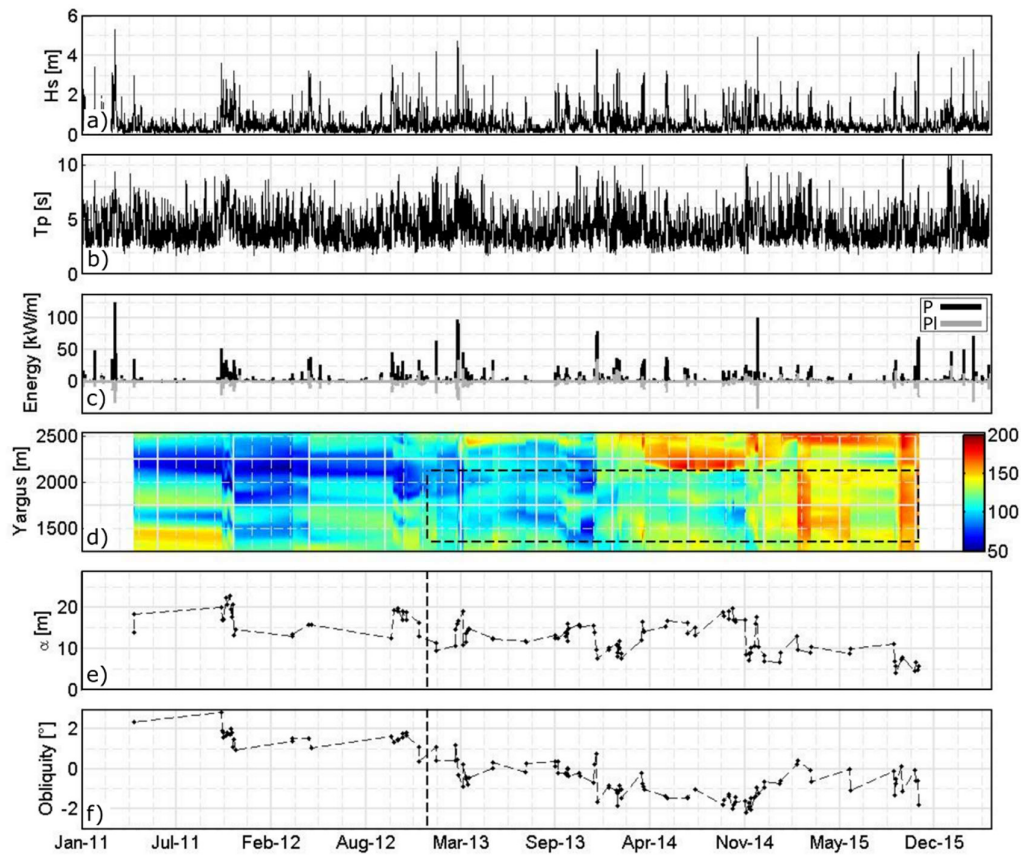
Figure 7. Temporal evolution of wave characteristics, offshore (a) Hs wave height, (b) peak period (Tp) and (c) energy. (d) Temporal evolution of inner-bar alongshore position in the NE sector. (e) Temporal evolution of sandbar three-dimensionality and (f) obliquity. Black shaded line represents the extremities of breakwater and the deployment period.

4.3.2. Crosshore sandbar response on the adjacent coast

Figure 8b presents the temporal evolution of the alongshore-averaged sandbar position with discrimination of the 2 sectors (behind breakwater and on the adjacent coast). Figure 8 is given with the time series of Hs wave height. Although at a different mean distance to the shore, the inner bars at the SE and SW sectors show similar behavior prior to the deployment. The overall sandbar position was reasonably stable in both sectors, showing short-term higher variability during storm events. After the submerged structure deployment, a series of storms in March 2013 led to a strong offshore migration of the bar at both sectors. However, in contrast with prior to the deployment, the offshore migration was larger in the SW sector than in the NE sector by approximately a factor 2, with the inner bar of the SW sector remaining at about the same location during the subsequent months. During the subsequent winter, a major storm event with Hs peaking at 4.3 m occurred in December 2013 and drove another large (approximately 30 m) offshore migration event in the NE sector, which was increased to approximately 50 m in the SW sector. This event drove the splitting of the sandbar between the 2 sectors. As the bar in the SW sector migrated far offshore (approximately 275 m from the shore) and increased substantially in depth (cf. section 4.2), a new (inner) bar formed shoreward in the SW sector. This new inner bar welded to the bar in the NE sector to form a continuous and reasonably alongshore-uniform sandbar across the entire domain.

Mean beach width was also computed behind the submerged breakwater between Yargus = 1400 m and 2100 m. The temporal evolution is given in figure 8b. Before the structure deployment, the shoreline was retreating at a mean rate of 2 m/year shoreward of the submerged breakwater. Few months after the structure deployment near April 2013, beach widening of 20 m in one year. After July 2014, shoreline positions remained reasonably stable until beach nourishment in December 2014.
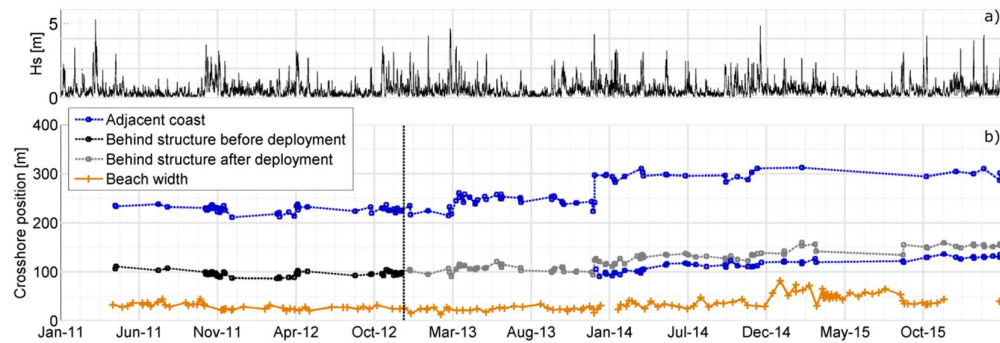
Figure 8. Temporal evolution of (a) the offshore Hs wave heights and (b) sandbars and shoreline crosshore positions with indication the deployment of the submerged structure in black shaded line.

5. Discussion and conclusion

At the lido of Sete, relatively slow NOM cycle has been observed (Certain, 2005, Aleman, 2013) but because of low temporal resolution, the role of single storm events in this process was difficult to quantified precisely (Gervais et al., 2012). Here, a very fast natural episodic net offshore migration has been observed in the SW sector on December 2013 with an offshore migration rate of 50 m/day. In line with a previous study (Ruessink et al., 2009) our investigation underlines the possible predominant role of episodic events on the onset of NOM cycles. Our study further highlight large alongshore difference in offshore migration rates as a result of the breakwater implementation. Sandbar splitting was observed during storm in December 2013 and it is hypothesized to be caused by the submerged breakwater that, through wave energy dissipation through depth-induced breaking across the structure, inhibits further offshore migration of the sandbar in the NE sector. This will need to be further proven through numerical modelling.

However, even if this split was clearly generated during the storm of December 2013, the progressive clockwise rotation of the initial oblique NE sandbar is observed since structure deployment and certainly played a role in the disconnection with the bar on the adjacent coast. Mechanisms driving the progressive reshaping of the tridimensional and oblique inner sandbar into an offshore-migrating alongshore-uniform ridge of sand remain unclear. Detailed process-based surf-zone sandbar morphodynamic modelling including the implementation of the submerged breakwater will be required to decipher the cause of these morphological changes.

The typical formation of a salient or tombolo was not observed and shoreline pursued its coupling with the inner bar, although the shoreline-sandbar system geometry was deeply changed. Since structure deployment, the morphology of the inner bar has changed drastically, and the beach widened by approximately 20 m. These results suggest a positive role of the submerged structure on the behavior of the aerial beach on the long term. In addition, during storms, a reduction in wave run-up was qualitatively observed through video timestacks in the alignment of the submerged breakwater. Previous experiments at the lido of Sete beach show that inner-bar and shoreline maintained a complex relationship (Balouin, 2013). Bar cusps and cuspate shoreline were usually out-of-phase (seaward budges in the shoreline in front of the bar horns) but depending of wave energy and incidence crescentic sandbar patterns could rapidly migrate longshore and shoreline cusps could be observed in-phase the nearshore sandbar. The impact of this behavior on the erosion of the dune is interesting asunder certain wave and nearshore morphology conditions, localized beach and dune erosion can be enforced by the nearshore morphology (Thornton, 2007; Castelle, 2015). After the structure deployment, we observed a linearization of both the bar and the shoreline, with absence of alongshore substantial alongshore variability in wave run-up. Accordingly, our results indicate that the influence of the submerged structure on the sandbar is a cornerstone to further understand the complexified shoreline response. But the main output of this study suggests that, on barred-beaches, the role of the sandbar is critical to shoreline response to the implementation of breakwaters, even a few kilometers away from the structure, which has been overlooked in previous studies.

Acknowledgements

References

Aleman, N., Robin, N., Certain, R., Barusseau, J.P., Gervais, M., 2013. Net offshore bar migration variability at a regional scale: Inter-site comparison (Languedoc-Roussillon, France). *Journal of Coastal Research*: Special Issue 65 - *International Coastal Symposium* Volume 2: pp. 1715-1720.

Balouin, Y., Tesson, J., Gervais, M., 2013. Cuspate shoreline relationship with nearshore bar dynamics during storm events – field observations at Sète beach, France. *Journal of Coastal Research*, Special Issue No. 65, p 440-445.

Balouin, Y., Rey-Valette, H., Picand, P. A., 2014. Automatic assessment and analysis of beach attendance using video images at the lido of Sète Beach, France. *Ocean & Coastal Management*, 102, 114-122.

BCEOM, 2001. General study for the protection and sustainable management of the Lido of Sète to Marseillan General. synth. (December 2001), p. 122 Report (in French).

Besio, G., Mentaschi, L., Mazzino, A., 2016. Wave energy resource assessment in the Mediterranean Sea on the basis of a 35-year hindcast. *Energy*, 94, 50-63.

Black, K., Mead, S., 2001. Design of the gold coast reef for surfing, beach amenity and coastal protection: surfing aspects. *Journal of Coastal Research*, Special Issue 29, 115-130.

Castelle, B., Turner, I.L., Bertin, X., Tomlinson, R., 2009. Beach nourishment at Coolangatta Bay over the period 1987-2005: Impacts and lessons, *Coastal Engineering*, 56, 940-950.

Castelle, B., Marieu, V., Bujan, S., Splinter, K.D., Robinet, A., Senechal, N., Ferreira, S., 2015. Impact of the winter 2013–2014 series of severe storms on a double-barred sandy coast: beach and dune erosion and megacusp embayments. *Geomorphology*, 238, 135–148.

Certain, R., 2002. Morphodynamique d'une côte sableuse microtidale à barres : le Golfe du Lion (Languedoc-Roussillon). Perpignan, France : University of Perpignan, Ph.D. thesis, 209p.

Certain, R. and Barusseau, J.P., 2005. Conceptual modeling of sand bars morphodynamics for a microtidal beach (Sète, France). *Bull. Soc. Geol.* France, 176(4): 343-354.

Gervais, M., Balouin, Y., Belon, R., 2011. Morphological response and coastal dynamics associated with major storm events along the Gulf of Lions Coastline, France. Geomorphology, 143–144 (0), 69-80.

Gómez Lahoz, M., and Carretero Albiach, J. C., 2005. Wave forecasting at the Spanish coasts. *Journal of Atmospheric & Ocean Science*, 10(4), 389-405.

Grunnet, N.M., Ruessink, B.G., 2005. Morphodynamic response of nearshore bars to a shoreface nourishment. *Coastal Engineering* 52, 119–137. doi:10.1016/j. coastaleng.2004.09.006.

Hamm, L., Capobianco, M., Dette, H.H., Lechuga, A., Spanhoff, R., Stive, M.H.F. (2002). A summary of European experience with shore nourishment. *Coastal Engineering*, 47, 237-264.

Holland, K.T., Holmann, R.A., Lippmann, T.C., Stanley, J. And Plant, N., 1997. Practical use of video imagery in nearshore oceanographic field studies. IEEE *Journal of Oceanic Engineering*, 22, 81-92.

Holman, R.A. and Stanley, J., 2007. The history and technical capability of Argus. Coastal Engineering, 54:477-491.

Lippmann, T.C. and Holman, R.A., 1989. Quantification of sand bar morphology: a video technique based on wave dissipation. *Journal of Geophysical Research*, 94, 995-1011.

Longuet-Higgins, M., 1970. Longshore current generated by obliquely incident sea waves. *Journal of Geophysical Research*, 75, 6778–6801.

Ranasinghe, R., Turner, I. L., Symonds, G., 2006. Shoreline response to multi-functional artificial surfing reefs: A numerical and physical modelling study. *Coastal Engineering*, 53(7), 589-611.

Ruessink, B.G., Pape, L., Turner, I.L., 2009. Daily to interannual cross-shore sand bar migration: observations from a multiple sand bar system. *Cont. Shelf Res.*, 29: 1663–1677.

Thornton, E.B., Sallenger, A.H. and MacMahan, J.H., 2007. Rip currents, cuspate shorelines and eroding dunes. *Marine geology*, 240 (1-4), 151-167.

W.I. van de Lageweg, K.R. Bryan, G. Coco, B.G. Ruessink, 2013. Observation of shoreline–sandbar coupling on an embayed beach. *Marine Geology*, 344, pp. 101–114.